

Internal Noises in MOS/EIS, MOSFET/ISFET Structures and Light Addressable Potentiometric Sensors

Ferdinand GASPARYAN and Vladimir AROUTIOUNIAN

Department of Physics of Semiconductors & Microelectronics, Yerevan State University,
1 Alex Manoogian St., 0025 Yerevan, Armenia
Tel.: (37410) 55 55 902
E-mail: fgaspar@ysu.am

Received: 25 November 2011 /Accepted: 14 February 2012 /Published: 28 February 2012

Abstract: The main types of internal noises in (bio-) chemical sensors on the base of electrolyte-insulator-semiconductor structures, ion selective field-effect transistors and light addressable potentiometric sensors, are classified. Corresponding detailed electrical equivalent schemes are modeled and designed; expressions for noise spectral density are developed. The sources of the main types are shortly characterized. *Copyright © 2012 IFSA.*

Keywords: Sensor, Field-effect, Noise, Equivalent scheme.

1. Introduction and Definition of Noises

Main types of semiconductor based bio-(chemical) sensors operate using peculiarities and possibilities of field-effect, especially properties of depletion layer (DL) on the semiconductor-other media interface. Those are field-effect sensors: metal-insulator/oxide-semiconductor (MIS, MOS) and electrolyte-insulator-semiconductor (EIS) structures, light addressable potentiometric sensors (LAPS). It is obvious that sensitivity and selectivity of electronic devices, particularly sensors, are determined in general by the internal noises types and its level. Voltage (or current) noise spectral density (NSD) S_V (or S_i) usually are presented by the average square of the fluctuating voltage (root means square value) $\overline{V^2}$, or by the fluctuating current $\overline{i^2}$:

$$\overline{V^2} = S_V \Delta f, \quad \overline{i^2} = S_i \Delta f. \quad (1)$$

Here Δf is the elementary frequency bandwidth over which the noise is considered (further we will assume $\Delta f = 1 \text{ Hz}$).

Fluctuating value (e.g. current $I(t)$) can be presented as the sum of none-fluctuating (i_0) and fluctuating ($i(t)$) components:

$$I(t) = i_0 + i(t). \quad (2)$$

Then NSD will be determined as

$$S_V = \lim_{T_t \rightarrow \infty} \left(\frac{1}{2T_t} \left| \int_{-T_t}^{+T_t} I(t) e^{j2\pi ft} dt \right|^2 \right). \quad (3)$$

Here T_t is the long time period, f is the frequency, t is the current passage time.

While the noise is usually regarded as an undesirable property of materials for applications, the fluctuation phenomena contain important information about the material performance and may be utilized as a valuable method for characterization of semiconductor materials and devices for identification and exact quantitative description of the (bio-) chemical species in electrolyte medium. Noise spectroscopy is a powerful method also for studying the transport properties, performance and reliability of materials and devices. It should be noted that many standard methods of the material study like utilization of Hall effect, photoconductivity measurements, capacitance-voltage characteristics became not effective for the large group of materials and devices, especially for nanoscaled materials and devices. At the same time, noise spectroscopy is even more sensitive method for study the objects with scaling their sized down to nanoscale. The tools to extract and analyze the information are power spectra or noise spectral density. Presently, flicker-noise spectroscopy can be applied to several types of problems:

- ✓ Determination and characterization of the dynamics or structural features of materials;
- ✓ Determination and characterization of the transport phenomena of individual materials;
- ✓ Determination of flow dynamics in distributed systems based on the analysis of dynamic correlations in stochastic signals that are simultaneously measured at different points in space.

In this paper, the main types of internal noises in above-mentioned structures are classified. Corresponding detailed electrical equivalent schemes are modeled and designed, expressions for NSD are developed. Analyses show that main types of noises in chemical and bio-sensors can be classified as diagram in Fig. 1 [1-4]. Below we will shortly characterize the NSD and sources of the main types of those noises.

2. Specification of Noises

Thermal noise conditioned by the carrier's chaotic thermal motion. An accurate calculation based on a quantum mechanics model gives

$$S_V^T(f) = 4Rhf \left(\frac{1}{2} + \frac{1}{e^{hf/kT} - 1} \right), \quad (4)$$

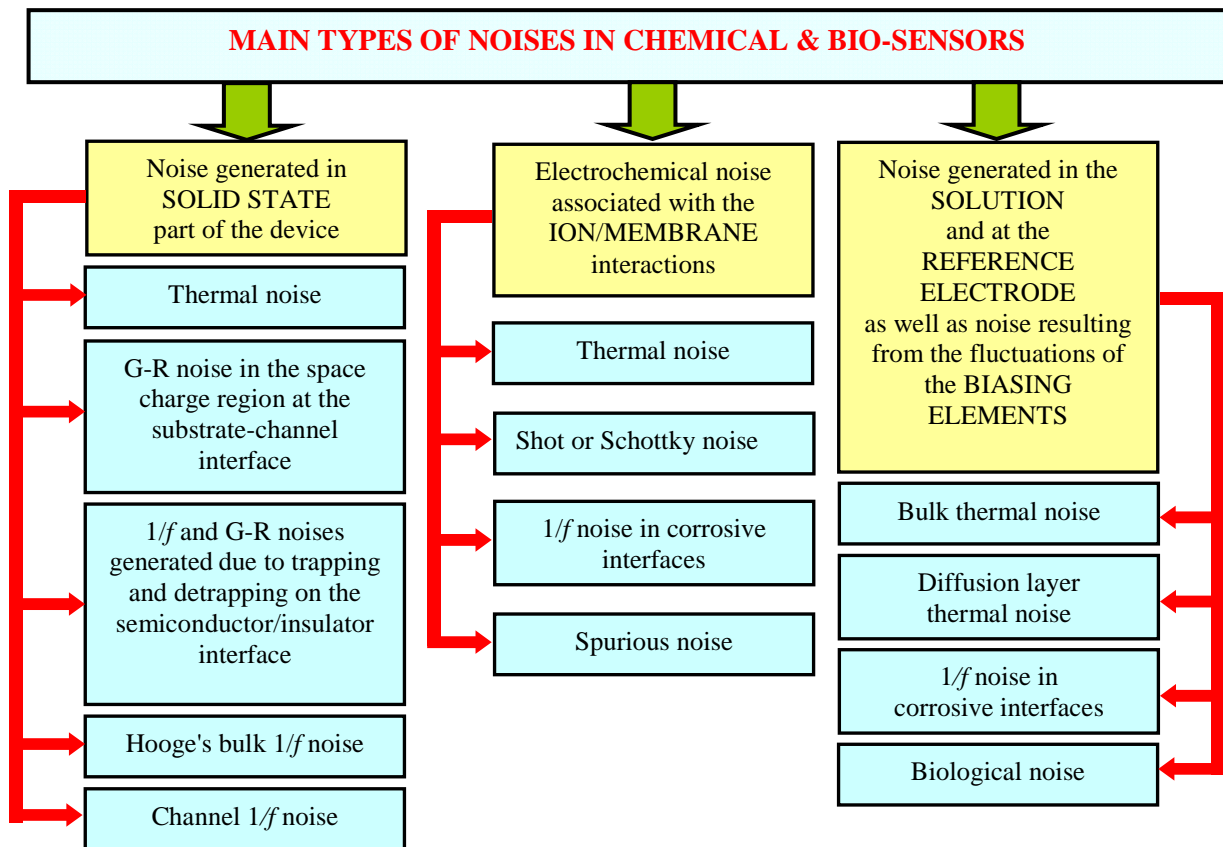


Fig. 1. Main types of noises in chemical and bio-sensors.

where R is the resistance of the sample. For “low” frequencies and high temperatures ($hf \ll kT$) we have frequency independent **white noise** and

$$S_V^T \approx 4kTR.$$

Generation-recombination noise can be understood by considering a semiconductor with a number of traps. The continuous trapping and de-trapping of the charge carriers causes a fluctuation in the number of carriers in the conduction and valence bands. The noise spectral density is Lorentzian in nature, with a corner frequency given by τ_n , the lifetime of the electrons in the conduction band. The current noise density can be presented as

$$S_n(f) = \frac{\langle (\Delta n)^2 \rangle 4\tau_n}{[1 + (2\pi f \tau_n)^2]}, \quad (5)$$

where $\langle (\Delta n)^2 \rangle \propto I^2$, I is the current. It should be noted that the corner frequency of this noise in observed spectra is dispersed, implying a wide distribution of lifetimes.

Biological noise conditioned by the fluctuation of the number of captured particles. Biological noise is very critical for regulating biological processes. Within each living cell, there are many “genetic circuits,” each composed of a distinct set of biochemical reactions that contribute to some biological process. Randomness in those reactions contributes to biological noise. Note that in a Lorentzian NSD with amplitude proportional to the number of particles in the solution is predicted [3].

Shot noise in electronic circuits is due to the quantized nature of the electric charge. It consists of random fluctuations of the electric current in a d.c. current due to that current actually consisting of a flow of discrete charges. Because the electron has such a tiny charge, however, shot noise is of relative insignificance in many (but not all) cases of electrical conduction. For instance, 1 A of current consists of about 6.24×10^{18} electrons per second; even though this number will randomly vary by several billion in any given second, such a fluctuation is minuscule compared to the current itself. Since shot noise is a Poisson process due to the finite charge of an electron, one can compute the root mean square current fluctuations as being of a magnitude $\sqrt{2eI\Delta f}$, and the spectral density is given by

$$S_i(f) = 2eI.$$

Here e is the elementary charge of an electron, and I is the d.c. current flow.

Low frequency (LF) or flicker noise conditioned by the random fluctuations of concentration or mobility (life times) of non-equilibrium carriers, ions and charged molecules, by the trapping and de-trapping processes on the surface and interface states, as well as by the electron-phonon interactions in the bulk of semiconductor and the fluctuation of electron's and phonon's distribution functions. Usually the time constants involved in the detection of chemical and biological species in an electrolyte medium via field effect are relatively large. Therefore it would be expected that **low frequency noise is more critical** than other types of noises in chemical and bio-FETs. Therefore, we will more detail discussed below low frequency noise mechanisms and its peculiarities.

For the field-effect based sensors, low frequency noises can be determined by the Hooge, McWhorter or charge fluctuation model. Usually in the FED-based sensors the semiconductor region mainly consists. Processes take place in those kinds of sensors mainly determined and described by the semiconductor part. On the Fig. 2 the main mechanisms of low-frequency $1/f$ noise in semiconductors are presented [5-10].

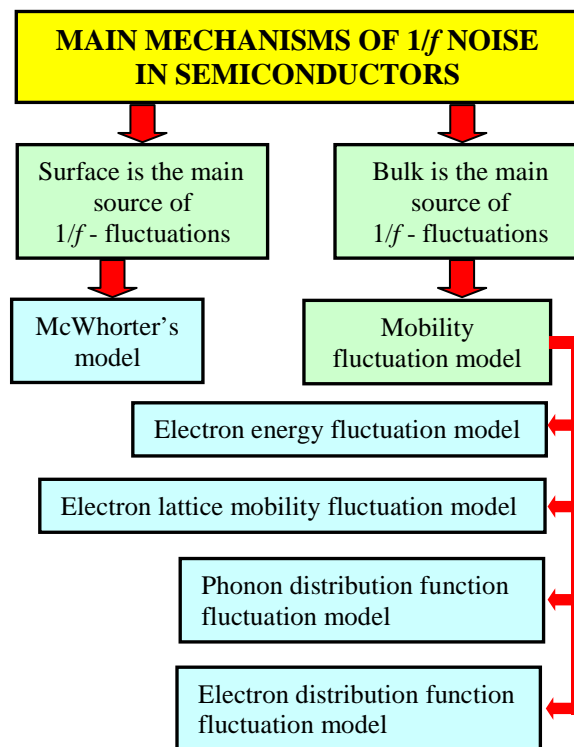


Fig. 2. Main mechanisms of $1/f$ noise in semiconductors.

For the field-effect based bio-chemical sensors NSD of low-frequency noises can be determined by the following models.

2.1. Hooge Model [11, 12]

The Hooge's universal formula for materials and structures with macroscopically homogeneous current density will be useful for modeling $S_i(f)$ dependencies barely [11]:

$$S_i(f) = \frac{\alpha_H I^2}{N_{tot} f^\gamma}, \quad (6)$$

where α_H is the Hooge's parameter (for semiconductors typically $\alpha_H \approx 2 \times 10^{-3}$ [11, 12], N_{tot} is the total number of electrons in the sample (means the total number of moving charges), magnitude of γ is close to 1. Unfortunately, the Hooge's formula does not give opportunity to take into account processes taking place in the electrolyte medium of the sensors made of EIS and ISFET structures [13].

2.2. McWhorter's or Correlated Number-mobility Fluctuation Model

In the correlated number-mobility fluctuation theory NSD of the flat-band voltage fluctuation can be described as [2]

$$S_{V,FB}(f) = \frac{e^2 k T N_t}{w l \beta C^2} \frac{1}{f}. \quad (7)$$

Here, w and l are width and length of the insulator gate, $\beta = \frac{2}{\hbar} \sqrt{2m^* \Phi_B}$ is the McWhorter's or tunneling parameter (m^* is the effective mass of electrons, Φ_B is the tunneling barrier height seen by electron at the interface), N_t is the oxide equivalent trap density in $\text{eV}^{-1} \text{cm}^{-3}$ C is the cumulative capacitance.

2.3. Charge Fluctuation Model

According to this model NSD can be calculated using the expression [14]:

$$S_V(f) = \frac{e^2 N}{w l C_{ef}^2} \frac{1}{f}. \quad (8)$$

Here N is the equivalent density of traps per unit area at the $\text{SiO}_2/\text{electrolyte}$ interface, $C_{ef} = \frac{C_i C_d}{C_i + C_d}$, C_i is the capacitance of the insulator layer and C_d is the capacitance of the semiconductor depletion layer.

Last two models can be successfully used for describing the LF noises in EIS and ISFET sensors.

For analyzing the noise properties, we need for model equivalent electrical scheme of the elements of investigated structures. Below we will be use the standard equivalent schematic analog of a noisy resistor R consisting of serial connected voltage generator via average square of the fluctuating voltage $\overline{V^2}$, or by the parallel connected current generator via average square of the fluctuating current $\overline{i^2}$ (Fig. 3).

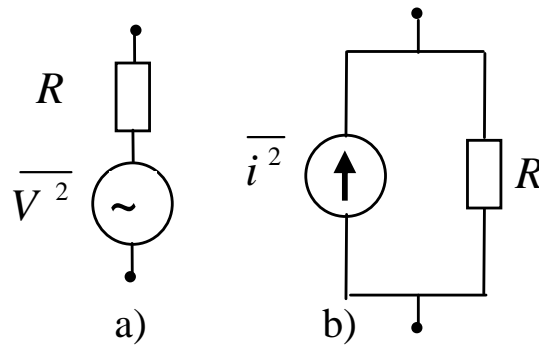


Fig. 3. Equivalent schematic analogy of a noisy resistor.

3. Noises Sources and Equivalent Electrical Schemes

3.1. EIS (MIS, LAPS) Structures

The EIS schematic picture is presented in Fig. 4a. Note that interchanging in a EIS structure, DNA layer, electrolyte and reference electrode by the metallic layer we will get ordinary MIS structure, and by the adding the LED (light emitting diode) to EIS structure we will get LAPS. On the base of detailed analyses of several properties of this structures (see, e.g. [1, 2, 14]) the electrical scheme for noises analyses for the case of the presence of DNA layer can be presented as in Fig. 4b. On Fig. 4b electrical scheme for MIS structure is show by the dashed green zone in the right. By the dashed red zone in the left additional current noise source for LAPS is shown. Electrical and other characteristics of MIS-like structures are detailed investigated also in [12]. Noise sources presented in Fig. 4b are: $\overline{V_s^2}$ is the semiconductor

$$\overline{V_s^2} = 4kTR_{Sb} + \frac{4kTR_{Sd}}{1 + (\omega R_{Sd} C_d)^2}; \overline{V_{FB}^2} = \frac{e^2 k T N}{\gamma \omega I C_{ef}^2} \frac{1}{f}; \overline{V_i^2} = 4kTR_i; \overline{V_{DNA}^2} = \frac{K_D V_D^a}{f^b}; \quad (9)$$

$$\overline{V_b^2} = 4kTR_b; \overline{V_D^2} = 4kTR_D; \overline{V_{RE}^2} = 4kTR_{RE}; R_S = R_{Sb} + R_{Sd},$$

$\overline{V_s^2}$ and $\overline{V_i^2}$ are the semiconductor and insulator bulk resistance voltage noise sources, correspondingly, $\overline{V_{FB}^2}$ is the noise source conditioned by the flat-band voltage fluctuation, R_{Sb} and R_{Sd} are resistivities of the bulk region and depletion layer of the semiconductor, correspondingly.

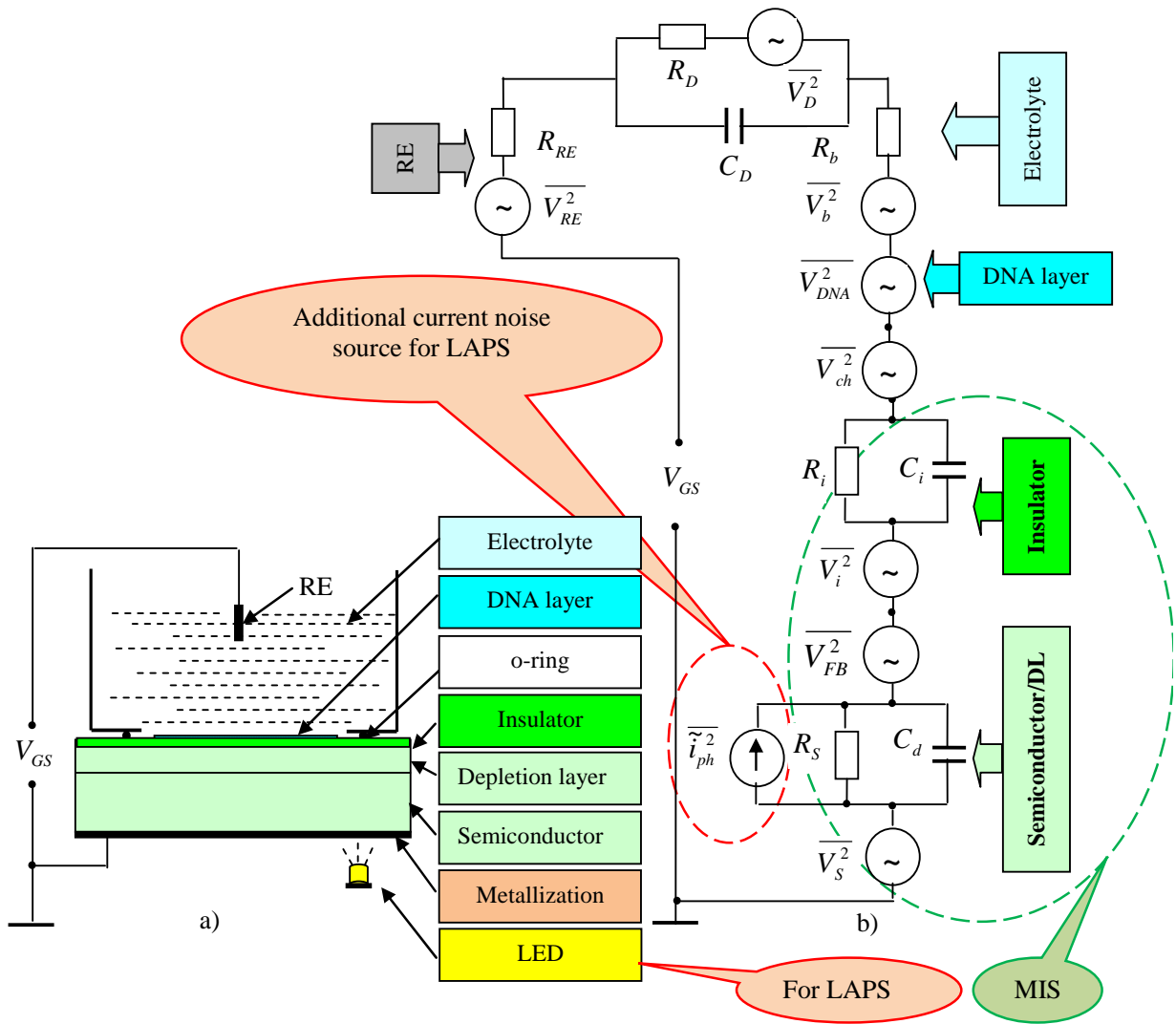


Fig. 4. Schematic picture of EIS structure (a) and electrical scheme for noise analyses (b).

Note that second term in right hand of $\overline{V_s^2}$ is the g-r part of the noises, conditioned by the g-r processes in the depletion region. R_s and R_i are the bulk resistances, correspondingly, for semiconductor and insulator, C_d and C_i are the capacitances, correspondingly, for semiconductor depletion layer and insulator, $\overline{V_{ch}^2}$ is the spectral density of the charge fluctuation on the insulator/electrolyte interface [15], $\overline{V_D^2}$ is the spectral density of the thermal noise of charge transfer resistance fluctuations; R_D is the charge transfer resistance across electrolyte, $\overline{V_{RE}^2}$ is the spectral density of the thermal noise of the reference electrode resistance fluctuations, R_{RE} is the resistance of reference electrode. $\overline{V_b^2}$ is the bulk electrolyte R_b resistance fluctuation noise. The electrolyte resistance can be approximated by the spreading resistance $R_b \approx \frac{1}{K} \sqrt{\frac{\pi}{wl}}$ is the bulk electrolyte resistance, K is the electrolyte conductivity [2]. The noise source $\overline{V_{DNA}^2}$ represents an anticipated noise source, V_D is the potential on the DNA layer, K_D is the some parameter, a and b are some exponents [2]. This is due to the random motion of the immobilized DNA probes within the electrolyte. This motion can couple to the semiconductor channel and cause random fluctuations in the carriers. It is

expected that this noise source would depend on the potential across the DNA layer, since a higher potential could potentially further immobilize the probes and cause less noise.

Total noise for the MIS structure can be presented as (taking into account that $R_i \gg R_S$)

$$\overline{V_{MIS}^2} = \overline{V_S^2} + \overline{V_i^2} + \overline{V_{FB}^2} \approx 4kTR_i + \frac{e^2 kTN_t}{\gamma w l C_{ef}^2} \frac{1}{f} + \frac{4kTR_{Sb}}{1 + (\omega R_{sd} C_d)^2}. \quad (10)$$

For the EIS structure we can write (taking into account that $R_i \gg R_S + R_b + R_D + R_{RE}$):

$$\overline{V_{EIS}^2} \approx 4kTR_i + \frac{K_D V_D^a}{f^b} + \frac{e^2 N}{w l C_{ef}^2} \left(1 + \frac{kTN_t}{\gamma N} \right) \frac{1}{f} + \frac{4kTR_{Sb}}{1 + (\omega R_{sd} C_d)^2}. \quad (11)$$

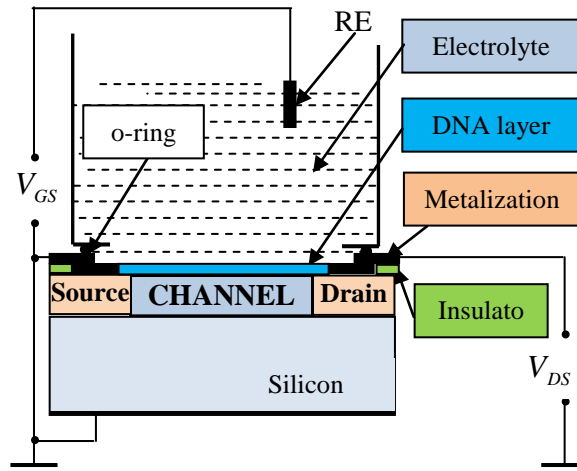


Fig. 5. MOSFET/ISFET schematic picture.

Schematic difference between the LAPS and EIS is the additional irradiation local source. Fluctuation of the leakage current conditioned by the photo-generated extra carriers in the LAPS can be presented on the equivalent scheme by the new current noise source \tilde{i}_{ph}^2 , connected parallel with R_S (Fig. 4b, red color segment). As it is shown in [9], the a.c. component of the photocurrent density \tilde{i}_{ph} is equal to

$$\tilde{i}_{ph} = \frac{\omega C_d}{\sqrt{1 + (\Omega \tau)^2}} \frac{e \tau d W}{\varepsilon_0 \varepsilon_s h \nu} (1 - e^{-\alpha d}). \quad (12)$$

Here ε_0 is the vacuum electric permittivity, ε_s is the relative dielectric constant of semiconductor, α is the irradiation absorption coefficient, W is the incident irradiation power density, d is the thickness of the semiconductor depletion layer, $h\nu$ is the quantum energy, Ω is the irradiation modulation frequency. Then we can present NSD for the LAPS as a sum of sources expressed by the Eq. (11) and additional components

$$\overline{V_{ph}^2} = \Delta R^2 \overline{\tilde{i}_{ph}^2} + \frac{4kT \Delta R}{1 + (\omega \tau)^2}. \quad (13)$$

First term characterized noise source conditioned by the additional fluctuation of the semiconductor bulk resistance ΔR under irradiation, second term is the g-r part of additional photo-carriers. Then, we get for LAPS

$$\overline{V_{LAPS}^2} \approx 4kTR_i + \frac{K_D V_D^a}{f^b} + \frac{e^2 N}{wLC_{ef}^2} \left(1 + \frac{kTN_i}{\gamma N} \right) \frac{1}{f} + \frac{4kTR_{sb}}{1 + (\omega R_{sd} C_d)^2} + \Delta R^2 \overline{i_{ph}^2} + \frac{4kT\Delta R}{1 + (\omega\tau)^2}. \quad (14)$$

3.2. MOSFETs (ISFETs)

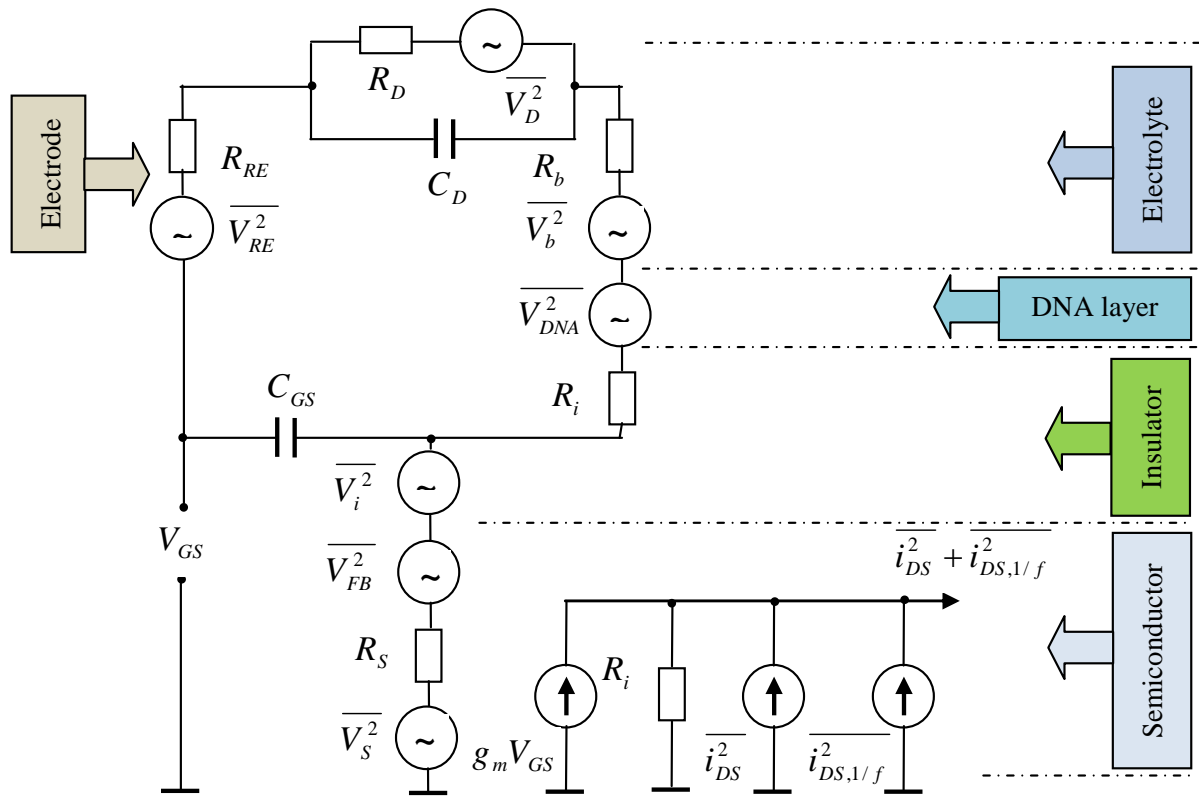
Schematic picture and equivalent electrical scheme of the MOSFET/ISFET structure are presented on Figs. 5 and 6, correspondingly (for the case of the non-Faradaic electrode on Fig. 6a, for the case of the Faradaic electrode on Fig. 6b). Here V_{GS} and V_{DS} are gate-source and drain-source applied voltages. In difference of EIS (MIS, LAPS) structures having only vertical current “channel” (Metal-Semiconductor-Insulator-Electrolyte-RE), in MOSFET/ISFET structures accrue also horizontal source-drain current “general channel” (Source-Channel-Drain). Basically source-drain current noise is Hooge’s $1/f$ noise, flat-band voltage fluctuation noise, semiconductor potential and depletion region resistance fluctuation noise. According to Haartman and Osting [16]:

$$\overline{i_{DS}^2} = \frac{\overline{i_{Ch}^2} + g_{Ch}^2 R_{SD}^2 \overline{i_{R_{SD}}^2}}{[1 + g_{Ch}(R_{SD} + R_L)]^2}, \quad \overline{i_{DS,1/f}^2} = \frac{e\alpha_H \mu_{ef} i_{DS} V_{DS}}{l^2 f}. \quad (15)$$

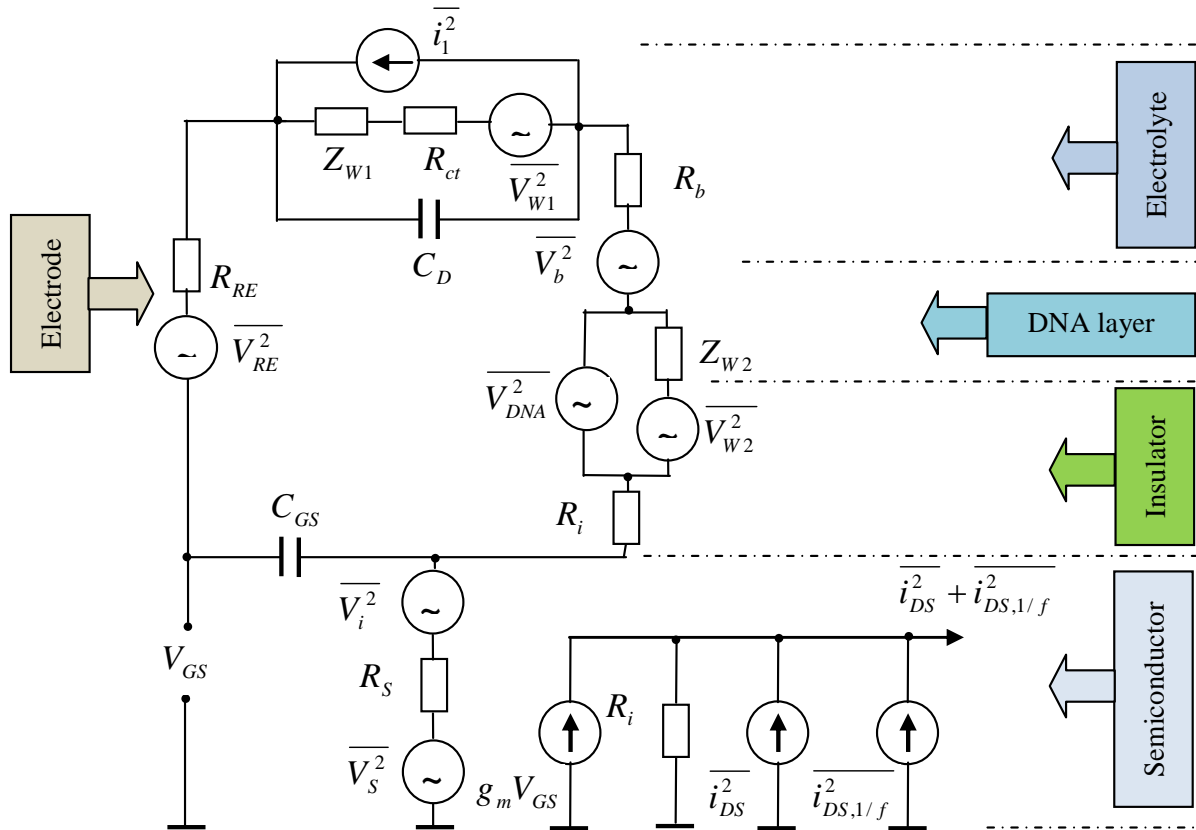
In (15) $\overline{i_{Ch}^2}$ is the noise contribution from the channel with conductance g_{Ch} , μ_{ef} is the effective carrier mobility, R_L is the load resistor resistance; $\overline{i_{R_{SD}}^2}$ is the low-frequency noise source operating from the drain-source access series resistances R_{SD} .

4. Conclusion

As we can see, noise spectral density for all field effect based (bio-)chemical sensors consists of three obligatory components: thermal, low-frequency and generation-recombination ones. Depending on the special experiment conditions either type of noises will be dominate in the appointed frequency interval. For example, in EIS functionalized with multi-layers of polyamidoamine dendrimer and single-walled carbon nanotubes $1/f$ noise dominates over thermal noise lower than 10 Hz [14], drain current NSD for the silicon-on-insulator (SOI) pMOSFET biased back gate voltages $1/f$ noise dominates in the region up to 500 Hz [16], for ISFETs at the buffer solutions pH7 and pH10 above a corner frequency ~ 1 Hz up to 400 Hz the measured spectra correspond to $1/f$ noise and below this corner frequency the measured spectra correspond to $1/f^2$ for [15], in n- and p-channel dynamic-threshold MOSFETs on SOI substrate NSD has both quasi $1/f$ and Lorentzian spectra up to 10^4 Hz [17].



a) For the non-Faradaic electrode



b) For the Faradaic electrode

Fig. 6. Electrical scheme for MOSFET/ISFET noise analyses.

References

- [1]. M. J. Deen, M. W. Shinwari and J. C. Ranuarez, Noise considerations in field-effect biosensors, *J. Appl. Phys.*, Vol. 100, 2006, pp. 074703.
- [2]. A. Hassibi, R. Navid, R. W. Dutton, T. H. Lee, Comprehensive study of noise processes in electrode electrolyte interfaces. *J. Appl. Phys.*, Vol. 96, 2, 2004, pp. 1074-1082.
- [3]. A. Hassibi, S. Zahedi, R. Navid, R. W. Dutton, and T. H. Lee, Biological shot-noise and quantum-limited signal-to-noise ratio in affinity-based biosensors. *J. Appl. Phys.*, Vol. 97, 2005, pp. 084701.
- [4]. F. V. Gasparyan, Photoresponse of LAPS with different species membranes: Modeling and simulation. *Sensors and Transducers*, Vol. 111, 12, 2010, pp. 141-154.
- [5]. S. V. Melkonyan, F. V. Gasparyan, V. M. Aroutiounian and C. E. Korman, Current carrier mobility fluctuations in homogeneous semiconductors, in *Proc. of the SPIE's 1st Int. Symp. on Fluctuation and Noise*, 1-4 June 2003, Santa Fe, New Mexico, USA, Vol. 5115, 2003, pp. 412-420.
- [6]. S. V. Melkonyan, V. M. Aroutiounian, F. V. Gasparyan and C. E. Korman, Peculiarities of electron distribution function's fluctuations damping in homogeneous semiconductors, *Physica B: Physics of Condensed Matter*, Vol. 357, 3-4, 2005, pp. 398-407.
- [7]. S. V. Melkonyan, V. M. Aroutiounian, F. V. Gasparyan and H. V. Asriyan, Phonon mechanism of mobility equilibrium fluctuation and properties of 1/f-noise, *Physica, B: Physics of Condensed Matter*, Vol. 382, 1-2, 2006, pp. 65-70.
- [8]. S. V. Melkonyan, F. V. Gasparyan and H. V. Asriyan, Main sources of electron mobility fluctuations in semiconductors, in *Proc. of the SPIE's 4th Int. Symp. on Fluctuation and Noise*, 20-24 May 2007, Florence, Italy, 2007, Vol. 6600, pp. 66001K.
- [9]. F. V. Gasparyan, S. V. Melkonyan, V. M. Aroutiounyan and H. V. Asriyan, 1/f Noises of homopolar and heteropolar semiconductors, *Int. J. Mod. Phys. B (IJMPB)*, Vol. 14, 7, 2000, pp. 751-760.
- [10]. H. V. Asriyan and F. V. Gasparyan, 1/f Noise component conditioned by built-in electric field in semiconductors, *Modern Physics Letters B*, Vol. 18, 10, 2004, pp. 427-442.
- [11]. F. N. Hooge, T. G. M. Kleinpenning and L. K. J. Vandamme, Experimental studies on 1/f noise, *Rep. Prog. Phys.*, Vol. 44, 1981, pp. 479-532.
- [12]. K. K. Hung, P. K. Ko, C. Hu and Y. C. Cheng, A unified model for the flicker noise in metal-oxide-semiconductor field-effect transistors, *IEEE Trans. ED*, Vol. 37, 1990, pp. 654-665.
- [13]. F. V. Gasparyan, A. Poghosyan, S. A. Vitusevich, M. A. Petrychuk, V. A. Sydoruk, J. R. Siqueira, O. N. Oliveira Jr., A. Offenhäuser and M. J. Schöning, Low-frequency noise in field-effect devices functionalized with dendrimer/carbon-nanotube multilayers, *IEEE Sensors Journal*, Vol. 11, 1, 2011, pp. 142-149.
- [14]. F. V. Gasparyan, S. A. Vitusevich, A. Offenhäuser and M. J. Schöning, Modified charge fluctuation noise model for electrolyte-insulator-semiconductor devices, *Mod. Phys. Lett. B (MPLB)*, Vol. 25, 11, 2011, pp. 831-840.
- [15]. C. G. Jacobson, M. Feinsod, Y. Nemirovsky, Low frequency noise and drift in ion sensitive field effect transistors. *Sensors and Actuators B*, Vol. 68, 2000, pp. 134-139.
- [16]. M. von Haartman and M. Osting, Effect of channel positioning on the 1/f noise in silicon-on insulator metal-oxide-semiconductor field-effect transistors, *J. Appl. Phys.*, Vol. 101, 2007, pp. 03456.
- [17]. J. Jomaah, F. Balestra and G. Ghibaudo, Low frequency noise in advanced Si bulk and SOI MOSFETs, *J. Telecomun. Inf. Techn.*, Vol. 1, 2005, pp. 24-33.